Resistance studies of overbank flow in rivers with sediment using the flood channel facility

Etudes menées au FCF (Flood Channel Facility) sur la résistance des écoulements avec débordement dans les rivières avec sédiments

DONALD W. KNIGHT, *PhD, CEng, MICE, MCIWEM, MASCE, School of Civil Engineering, The University of Birmingham, Edgbaston, Birmingham, B15 2TT, UK*

FENELLA A. BROWN, *BSc, PhD, Marine Sciences Laboratory, Menai Bridge, Bangor, Wales, UK*

ABSTRACT
Some large scale experiments concerning equilibrium sand channels with overbank flow are described. The experiments were undertaken in the UK Flood Channel Facility (FCF) configured into a straight compound channel with fixed banks, a mobile main channel composed of uniform sand with a d50 of around 0.8mm, and two symmetric floodplains. The main channel alluvial resistance changed with flow depth and discharge in a complex way arising from the effects of both bedforms and the floodplain/main channel interaction processes. Overall, zonal and local resistance coefficients for this type of channel are reviewed and the data discussed in relation to practical modelling of alluvial channels with overbank flow.

RÉSUMÉ
Quelques expériences à grande échelle concernant la stabilité des canaux sableux avec débordement sont décrites ici. Les expériences ont été entreprises dans l'installation britannique FCF dédiée aux chenaux d'inondation, configurée en un canal rectiligne à bords fixes, composé d'un chenal principal en sable de granulométrie uniforme avec un d50 d'environ 0.8 mm, et de deux plaines d'inondation symétriques. La résistance alluviale du canal principal variait avec le tirant d'eau et le débit d'une manière complexe due à la fois aux formes de lits et aux interactions lit mineur/lit majeur. Dans l'ensemble, les coefficients de frottement locaux et par zone pour ce type de canal sont passés en revue et les données sont discutées relativement à la modélisation pratique des chenaux alluviaux avec débordement.

1. Introduction

The UK Flood Channel Facility (FCF) is a large scale national facility for undertaking experimental investigations of overbank flows in rivers. It was constructed in 1986 to enable engineers to understand the hydraulic processes involved in the flood flows of rivers at high stage. The FCF has been used for overbank flow studies on straight, meandering and free formed channels with floodplains, with either rigid or mobile boundaries. Since the majority of hydraulic experiments involving sediment channels have been conducted with either inbank or bankfull discharges, these large scale experiments on overbank flow involving alluvial channels are therefore somewhat unusual.

In overbank flow the interaction between the floodplains and an alluvial river channel is considerably more complex than that for a non-erodible river channel, since the bedforms of the alluvial channel, and hence roughness, change with discharge or stage. Unlike rigid boundary channels, which have been researched extensively over the last 35 years (e.g. Sellin, 1964; Knight & Demetriou, 1983, Knight & Shiono, 1996), mobile bed channels have received relatively little attention, despite their relevance to practical river engineering problems such as river training and morphology, sediment transport, dredging and design of flood alleviation works. This paper, along with its two companion papers (Myers et al, 2000; Valentine et al, 2000), is an attempt at rectifying this dearth of information on overbank flow in this type of channel.

2. Experimental apparatus and procedures

2.1 The Flood Channel Facility

A general layout of the FCF is shown as Fig. 2 in the companion paper by Myers et al. (2001). The FCF is 60m long by 10m wide and can be configured to suit any type of rigid or mobile channel under investigation. For these experiments the valley floodplain slope was moulded to 1.834×10^{-3}, and a uniform sand was used as the sediment in the main river channel. The maximum discharge used was 0.75 m^3s^{-1}, somewhat less than the full capacity of the facility which was 1.1 m^3s^{-1}.

Most of the experiments were conducted with two 3.0m wide concrete floodplains, set 2.0m apart, thus giving a central main channel composed of a uniform sand with a d_{50} of 0.83mm. Reasons for this choice of sediment size are given in Knight et al (1999). The sand was laid to a depth of 750mm below floodplain level, in order to allow for the full development of bedforms, and screeded to a mean bed level 200mm below the floodplains. This then produced a main river channel with a trapezoidal cross section, a mobile bed width of 1.6m, two rigid sidewalls with 1:1 slopes, a top width of 2.0m, flanked by two symmetric flood plains, each 3.0m wide. The cross section was thus of a compound nature, as shown in a general view of the FCF in Fig. 1. For certain tests involving high inbank flows, temporary wooden sidewalls were added to the main channel to isolate the floodplains, as illustrated in Figs 1 & 4 of Knight et al (1999).

Revision received May 23, 2000. Open for discussion till December 31, 2001.

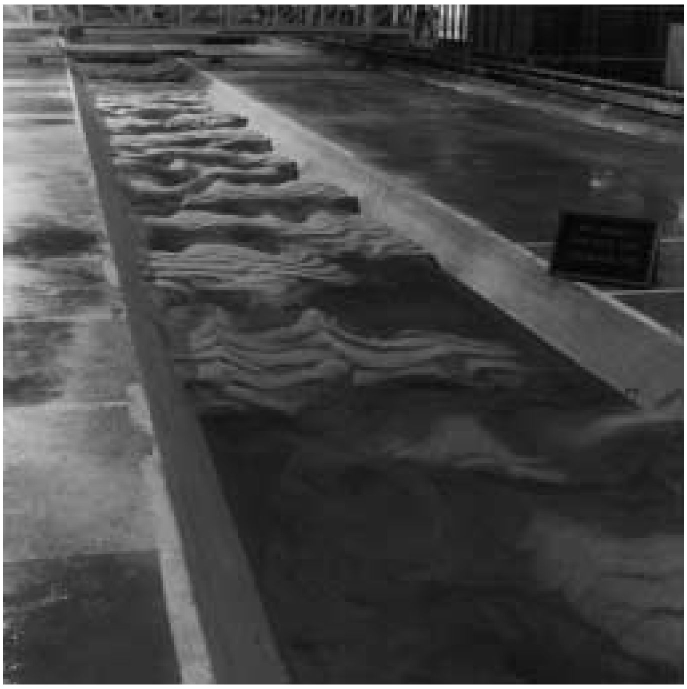

Fig. 1. Sand dunes for bankfull flow, Q = $0.175m^3s^{-3}$

The floodplains were either left with a relatively smooth concrete finish (denoted 'smooth' in later descriptions), as shown in Fig. 2, or roughened with 25mm diameter dowels at 12 dowels/m^2 (denoted 'rough'), as shown in Fig. 3. Following each experiment the bedforms in the main channel were surveyed and photographed. Fig. 1 shows typical bedforms following a bankfull discharge of $0.175m^3s^{-1}$, and Figs 2 & 3 show bedforms following a discharge twice that of bankfull, one with smooth floodplains and the other with both floodplains roughened with dowels. The size of these bedforms, their variation with discharge, the variation of roughness around the wetted perimeter and the shape of the compound channel are an indication of the difficulty of analysing such overbank flow in rivers. Full details of the apparatus and procedures are given in Brown (1997).

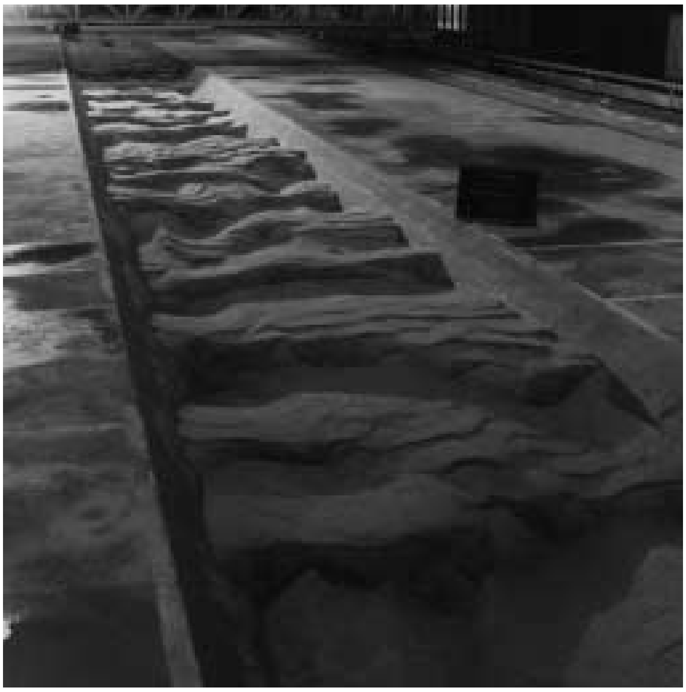

Fig. 2. Sand dunes for low overbank flow with smooth floodplains, Q = $0.350m^3s^{-3}$

Fig. 3. Sand dunes for low overbank flow with rough floodplains, Q = $0.350m^3s^{-3}$

Further details of the FCF and its programme of research may be found in Knight & Sellin (1987), in the discussion in the IAHR Journal following Knight & Shiono (1990), and in Knight et al. (1999). A general review of all the FCF experimental programmes, involving overbank flow studies in straight, skewed and meandering channels, is given elsewhere by Knight (1999).

2.2 Setting up procedures

Tables 1 & 2 summarise the main experimental parameters for the 26 experiments, 14 inbank flow experiments (or with wooden sidewalls added to isolate the main channel) and 12 overbank flow experiments, with either smooth or rough floodplains. Careful setting up procedures were required in order to obtain an equilibrium condition at the correct regime channel bed slope for each discharge, and these are described in detail in Knight et al. (1999). Not only did the tailgate settings have to be predetermined by a series of preliminary experiments, but even when equilibrium conditions had been established, the water surface slope and bedload rates had to be measured regularly in order to obtain a sufficiently long time series from which statistically sensible and accurate test values could be obtained. Figs 4 - 6 show typical variations in water surface slope, bedload rate and bed levels at one location to illustrate the dynamic nature of the 'equilibrium' channel. Experiments were sometimes run continuously for several days and nights in order to achieve satisfactory test conditions. Once an equilibrium condition was found, repeated measurements of the water surface slope were taken and averaged as shown in Fig. 5 in order to produce the values shown in Tables 1 & 2.

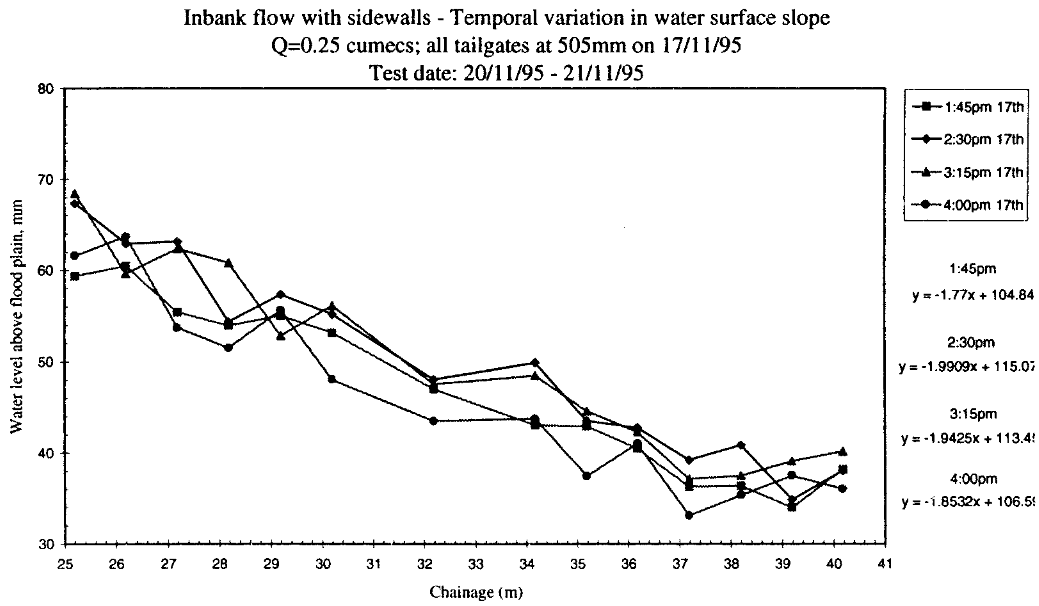

Fig. 4. Chart showing variation in water surface slope at one tailgate setting

The bedload was re-circulated from the downstream end of the main channel to the upstream end through a 75mm pipe, in which an infra-red meter was placed for recording the sediment concentration. These readings were supplemented by manual measurements of bedload taken directly at the downstream end of the main channel. Bed levels were monitored during the course of an experiment by an ultrasonic recorder, located at one position, 1.0m from the downstream end of the main channel, so that the bedload rate could be correlated with the dune migration rate, with an appropriate phase shift, as shown in Fig. 6. A complete survey of the bed was made at the conclusion of each experiment by means of an automatic bed level recorder. Typical examples of measured transverse bed profiles are shown in Figs 7 & 8 for discharges of 0.075 m^3s^{-1} (inbank flow) and 0.450 m^3s^{-1} (overbank flow). These demonstrate that the mean bed level stayed at 200mm below the floodplains throughout the experiment, indicating no net loss of sand in the re-circulating system.

2.3 Measurement of basic hydraulic parameters

The water depths were determined from the average of the readings of water surface slope for a given discharge. These data were then used to construct the stage-discharge curves for each type of channel configuration. Fig. 9 shows these three curves: for inbank flow in a trapezoidal channel (inbank and with sidewalls added at floodplain level to isolate the floodplains), overbank flow with smooth floodplains and overbank flow with rough floodplains. Equations through these data, and correlation coefficients, were obtained as:

$$\begin{array}{lll} \text{inbank, trapezoidal} & H=-0.9212Q^2+1.1629Q+0.0185 & R^2 = 0.9982 \\ \text{overbank, rough fp} & H=-0.1702Q^2+0.4125Q+0.1333 & R^2 = 0.9978 \\ \text{overbank, smooth fp} & H=-0.1557Q^2+0.3026Q+0.1536 & R^2 = 0.9931 \end{array} \quad (1)$$

where H is in m and Q is in m^3s^{-1}. These data were used together with the section geometry to give the overall or section average

Table 1. Summary of inbank flow experiments and overall resistance coefficients

Test date	Target Q (m^3s^{-1})	Actual Q (m^3s^{-1})	Average H (mm)	Slope S (x 1000)	Overall n	Overall f	Re ($x10^5$)	Fr
13/11/95	0.050	0.05055	70.77	1.80342	-	-	-	-
01/04/95	0.050	0.04894	70.76	1.76974	0.01654	0.05321	0.802	0.507
26/06/95	0.075	0.07496	105.09	1.79948	-	-	-	-
03/04/96	0.075	0.07454	96.66	1.66779	0.01772	0.05545	1.17	0.480
03/07/95	0.125	0.12460	155.17	1.59132	0.02279	0.07968	2.05	0.387
14/11/95	0.125	0.12550	156.03	1.70445	-	-	-	-
10/07/95	0.175	0.17324	200.80	1.72803	-	-	-	-
25/03/96	0.175	0.17565	198.78	1.60752	0.02459	0.08642	2.52	0.371
20/11/95	0.250	0.24989	252.57	1.71015	0.02667	0.09510	3.45	0.362
26/03/96	0.300	0.29996	278.59	1.63337	0.02563	0.08550	3.94	0.372
22/11/95	0.350	0.34873	311.18	1.78981	-	-	-	-
14/03/96	0.350	0.35028	309.52	1.75473	0.02720	0.09358	4.22	0.367
27/11/95	0.450	0.44875	356.64	1.81136	-	-	-	-
20/03/96	0.450	0.44894	358.09	1.90536	0.02836	0.09786	5.31	0.372

Table 2. Summary of overbank flow experiments and overall resistance coefficients

Test date	Target Q (m^3s^{-1})	Actual Q (m^3s^{-1})	Average H (mm)	Slope (x 1000)	Overall n	Overall f	Floodplain
estimate	0.175	0.17565	198.78	1.60752	0.01026	0.02336	rough
16/07/95	0.250	0.24762	227.31	1.80007	0.01690	0.05430	"
24/07/95	0.350	0.34978	258.11	1.76931	0.02138	0.07739	"
31/07/95	0.450	0.44953	281.44	1.84666	0.02385	0.09013	"
08/08/95	0.600	0.59887	320.18	1.84332	0.02788	0.11302	"
estimate	0.175	0.17565	198.78	1.60752	0.01026	0.02336	smooth
14/04/96	0.250	0.25004	224.93	1.48742	0.01439	0.03981	"
14/08/95	0.350	0.35000	246.31	1.77697	-	-	"
08/04/96	0.350	0.34754	239.02	1.88995	0.01583	0.04535	"
29/08/95	0.450	0.44992	261.78	1.79333	-	-	"
15/04/96	0.450	0.44825	256.90	1.77866	0.01640	0.04573	"
21/08/95	0.600	0.59840	278.35	1.84946	0.01721	0.04730	"
10/04/96	0.600	0.59776	269.89	1.71741	-	-	"
17/04/96	0.750	0.74800	293.47	1.92817	0.01703	0.04464	"

Manning and Darcy-Weisbach resistance coefficients shown in Tables 1 & 2.

In order to obtain local and zonal resistance coefficients in sub-areas of the compound channel it was necessary to measure the distribution of velocity and boundary shear stress across the FCF for every discharge. A typical set of velocity data, measured with a miniature propeller meter at 0.4 of the depth, is shown in Fig. 10 for an experiment with rough floodplains and a discharge of $0.350 m^3s^{-1}$. Measurements in the main channel were taken at three cross sections, 1m apart, in order to overcome the variability in the readings arising from the effect of the large bedforms, already shown in Figs 3 & 8. The floodplain measurements on the other hand were only made at one cross section, since the boundary was rigid. Although in the rough floodplain cases the wake from individual rod roughness elements affected these readings, as Fig. 10 shows, the mean value across each floodplain was easy to estimate for each discharge. A corresponding set of data for smooth floodplains, but with a higher discharge, is shown in Fig. 11. In this case the roughness of the main channel was so large that at this particular depth the floodplain velocities were comparable with the main channel velocities.

These depth-averaged velocity distributions, such as those shown in Figs. 10 & 11, were then integrated up laterally to give the proportion of the total discharge that occurred in either the main channel or on the floodplains. These proportions are prerequisites for any analysis of zonal resistance coefficients or alluvial bedforms in the main channel. Integration over the whole section was also undertaken in order to check that the total discharge was

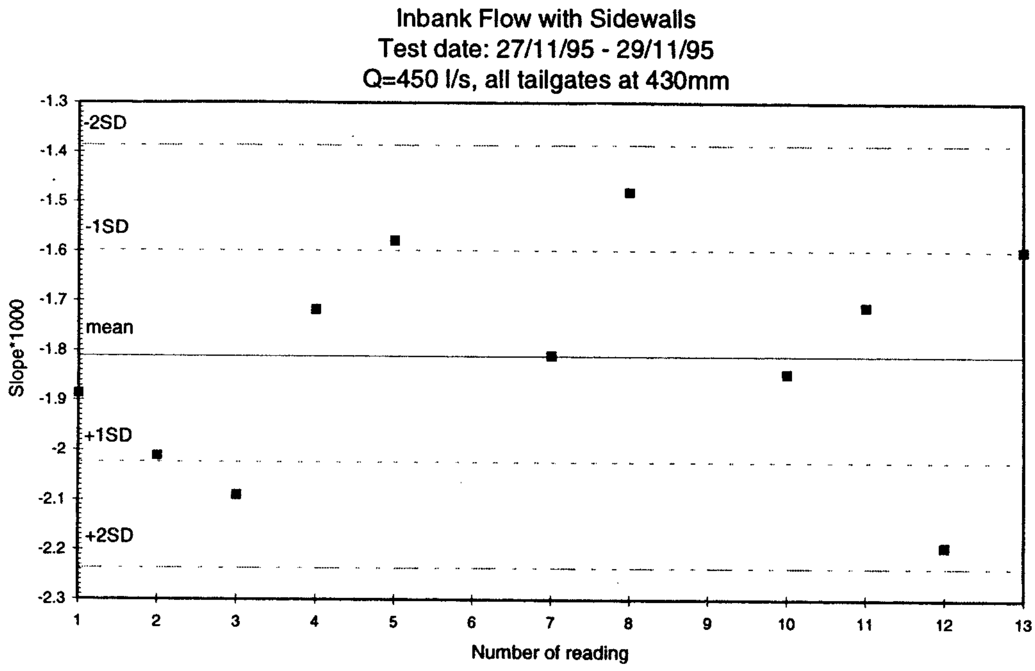

Fig. 5. Accepted estimates of slope for test BU271195 ($Q = 0.45 m^3s^{-1}$)

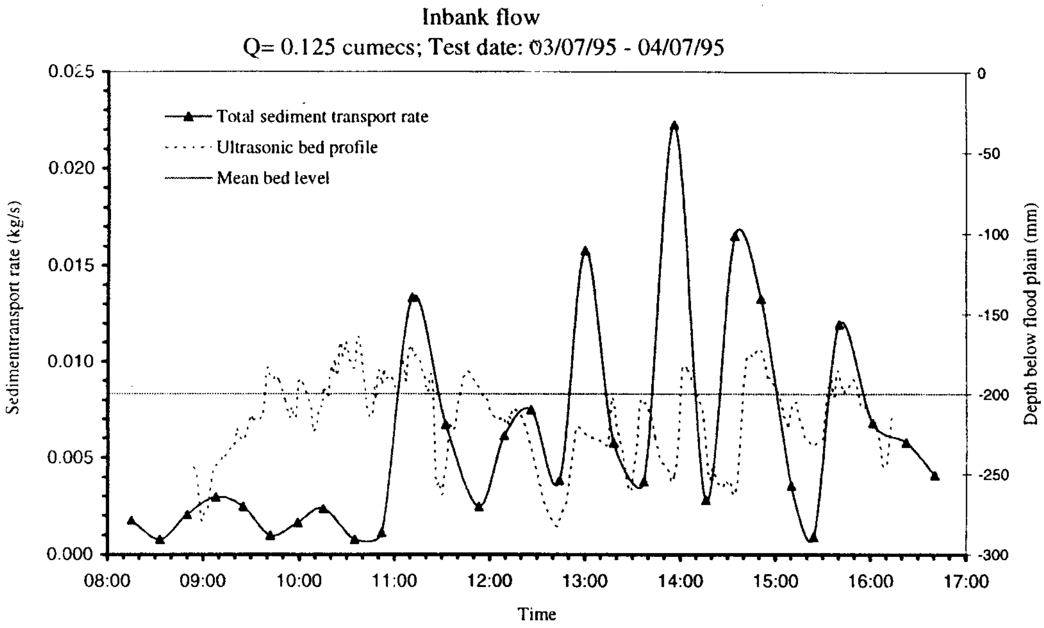

Fig. 6. Correlation between temporal variation in bed profile and manually measured sediment transport rate

of the same order as that given by the orifice plates monitoring the discharge supplied to the FCF. On account of the large bedforms in the main channel, and the variability in the velocity data within the main channel, the closing errors were larger than for rigid boundary systems (Knight, 1992).

Figs 12 & 13 show the results of these integrations, for each type of floodplain roughness, and how the proportion of the total discharge in the main channel, $\%Q_{mc}$, varies with depth. The main channel was taken to be the sub-area defined by two vertical interfaces drawn at the main channel/floodplain divide (at bankfull level). Also shown in each Figure is the variation of the area of the main channel, expressed as a percentage of the total channel cross section area, $\%A_{mc}$. The results are seen to composite well together, despite the data in some cases being measured many months apart. Tables 1 & 2 further show that where some experiments were repeated, the general level of repeatability and consistency is good.

3. Resistance analysis

3.1 Overall resistance coefficients

It is customary in one dimensional analysis to lump all hydraulic effects into a simple bulk flow resistance relationship, such as given by the Manning or Darcy-Weisbach equations:

$$Q = (AR^{2/3}S_f^{1/2})/n \quad (2)$$

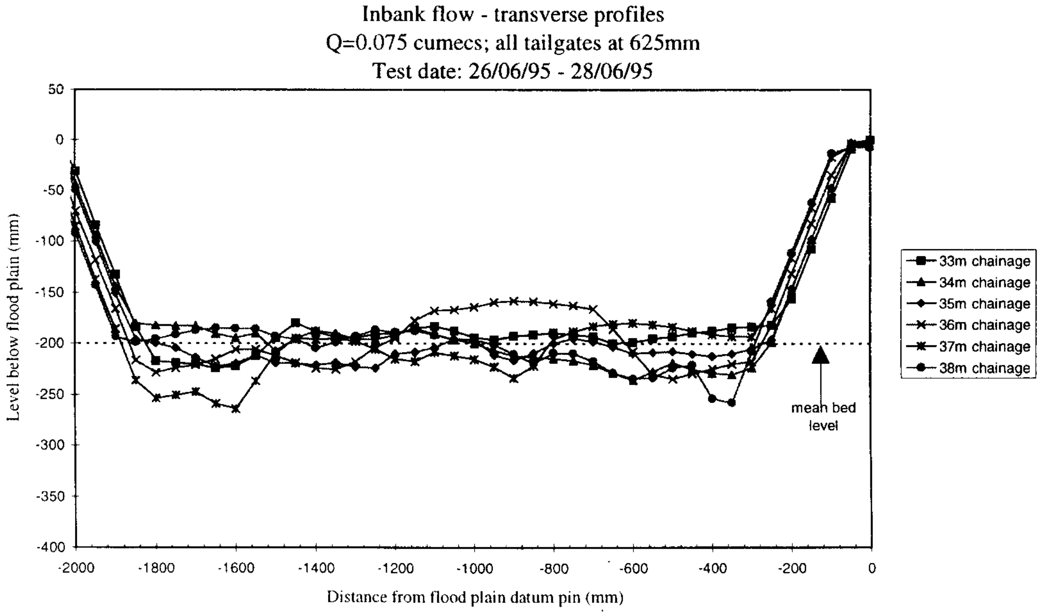

Fig. 7. Transverse bed profiles at 1m intervals over 5m of FCF test section, $Q = 0.075\ m^3s^{-1}$

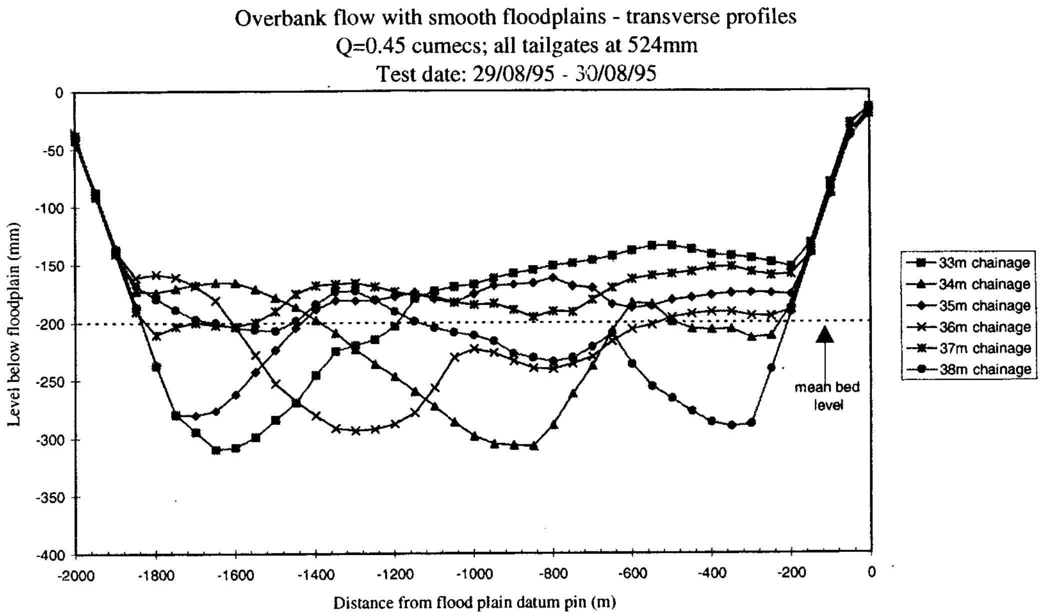

Fig. 8. Transverse bed profiles at 1m intervals over 5m of FCF test section, Q = 0.450 m^3s^{-1}

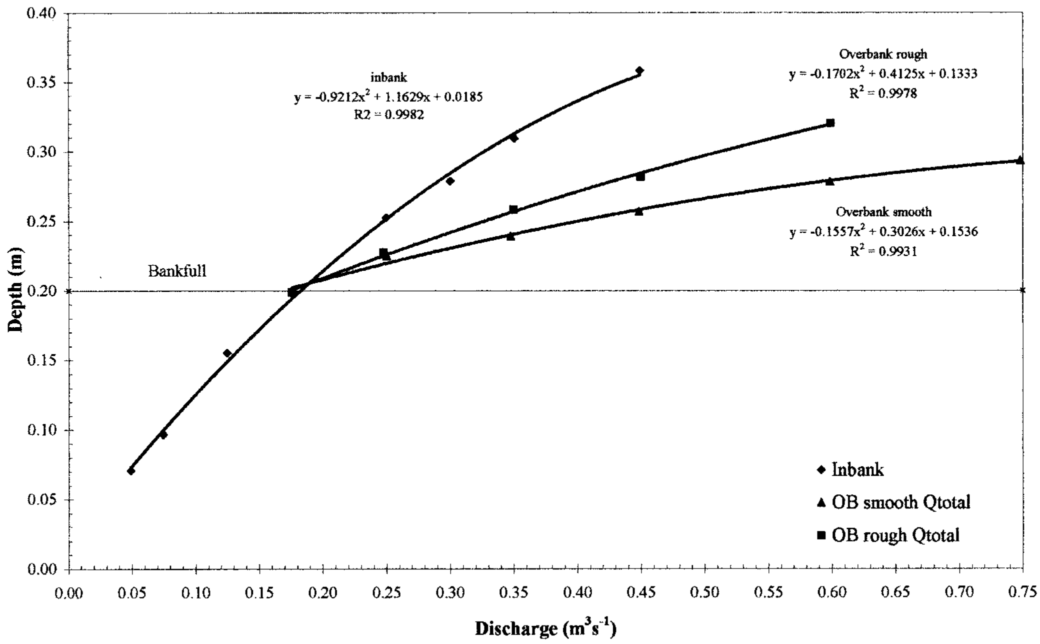

Fig. 9. Empirical stage-discharge relationships

$$Q = (8g/f)^{1/2} AR^{1/2} S_f^{1/2} \quad (3)$$

where Q is the discharge, A is the area, R is the hydraulic radius, S_f is the friction slope and n & f are resistance coefficients. It is known that f & n vary significantly with depth or discharge in most open channel flows, particularly so in natural sand bed rivers and estuaries (Knight, 1981; Wallis & Knight, 1984). The variation of the resistance coefficient, f, with Reynolds number and relative roughness is normally defined by the Colebrook-White equation. It should however be remembered that this 'standard' resistance equation is strictly only applicable to flow in circular pipes. Although it is frequently used for prismatic channels with simple shapes, it is not suitable for describing flows in channels with very complex cross sections. Despite this, the 'overall' or lumped Darcy-Weisbach and Manning resistance coefficients were evaluated from the stage-discharge data presented in Tables 1 & 2, treating the channel as a single section and using the actual measured water surface slopes rather than the floodplain valley slope.

The variation of these 'overall' f and n values with depth, H, are shown in Figs 14 & 15. Both graphs show that below bankfull, the resistance coefficients for inbank flow increase with depth as the height of the bedforms increase. The data labelled 'inbank', based on results from the 1.6m wide trapezoidal sand bed channel with two rigid wooden sidewalls isolating the floodplains, indicate how the f and n values increase with depth. The values nearly

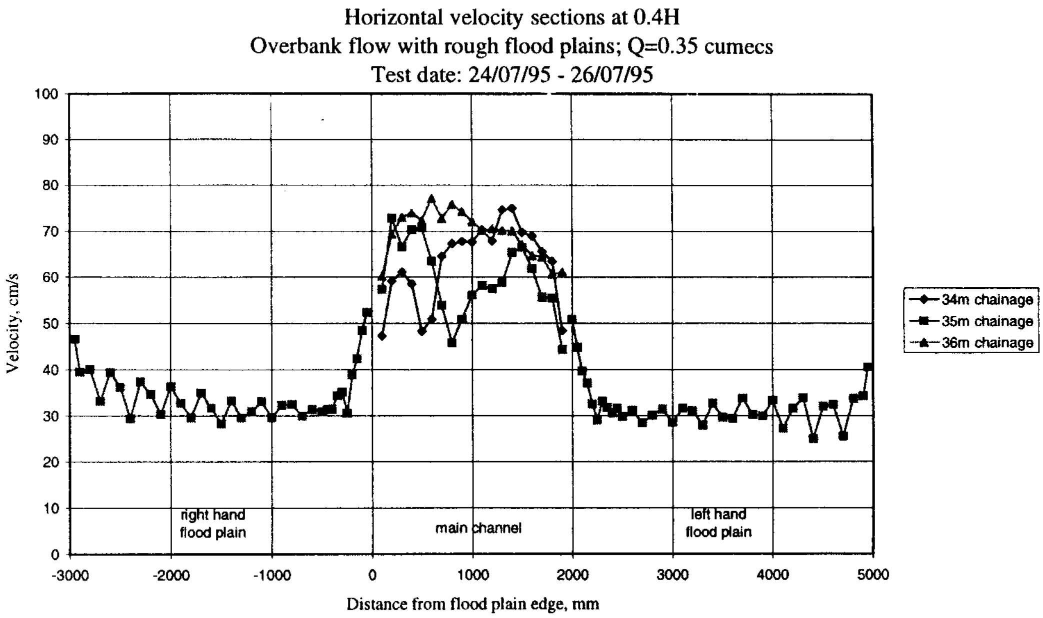

Fig. 10. Horizontal velocity traverse, 240795, Q = 0.35 m^3s^{-1} , rough floodplains

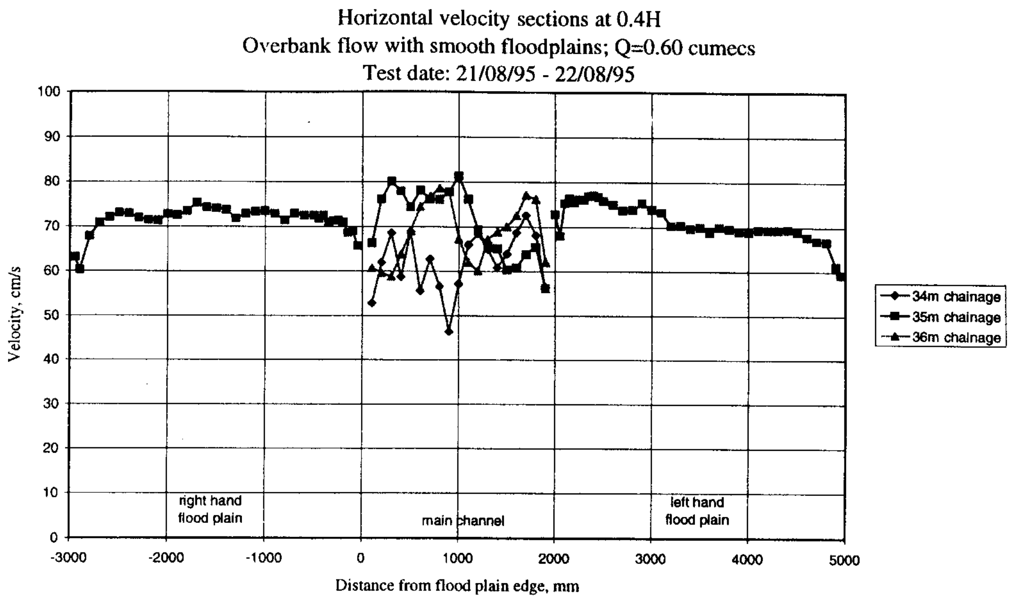

Fig. 11. Horizontal velocity traverse, 210895, Q = 0.60 m^3s^{-1} , smooth floodplains

double over the range of depths tested, indicating the increased form drag produced by the very large sand dunes. Preliminary analysis of bedform height and length, using the 5 methods listed by Nordin (1971), indicates that mean bedform height typically varied from 0.070 to 0.120 m and bedform wavelength from 0.7 to 1.90 m respectively. Data were collected over a 12 m length of the main channel, as illustrated elsewhere by Fig. 13 in Knight et al (1999). These bedforms cause the main channel resistance coefficients to increase with depth (and discharge), up to a more or less constant value, f = 0.110 and n = 0.030 at H = 0.40m, a depth slightly larger than those actually tested. However it should be remembered that although the height of the bedforms increases with discharge, as the depth increases, their influence becomes less as the length of the concrete and wooden sidewalls in contact with the water becomes a larger proportion of the overall wetted perimeter of the trapezoidal channel. The overall channel resistance coefficients shown in Figs 14 & 15 are therefore 'composite' values, produced by two different surfaces, one which varies with the flow and the other which does not (apart from Reynolds number effects), mixed in varying proportions as the flow depth increases. It should also be recognised that there are some scale effects related to these bed forms, arising from the fact that the d/H values are not scaled appropriately. Ancillary studies are being conducted at the University of Birmingham using a smaller compound sediment channel on this and related issues (Knight, Brown,Ayyoubzadeh & Atabay, 1999; Atabay & Knight, 1999). A characteristic feature of the overbank data presented in Figs 14 & 15 is the apparent reduction in overall resistance at the bankfull stage, due to the sudden decrease in hydraulic radius. The Darcy-Weisbach friction factor drops from a value of 0.0865 just below

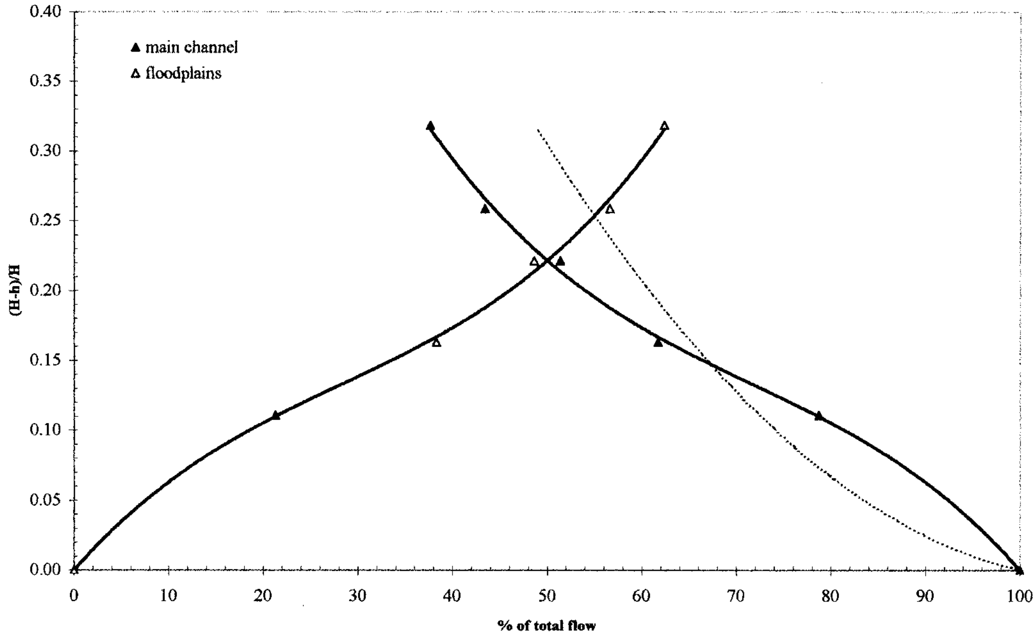

Fig. 12. Percentage of total flow in main channel, $\%Q_{mc}$, smooth floodplains, and $\%A_{mc}$

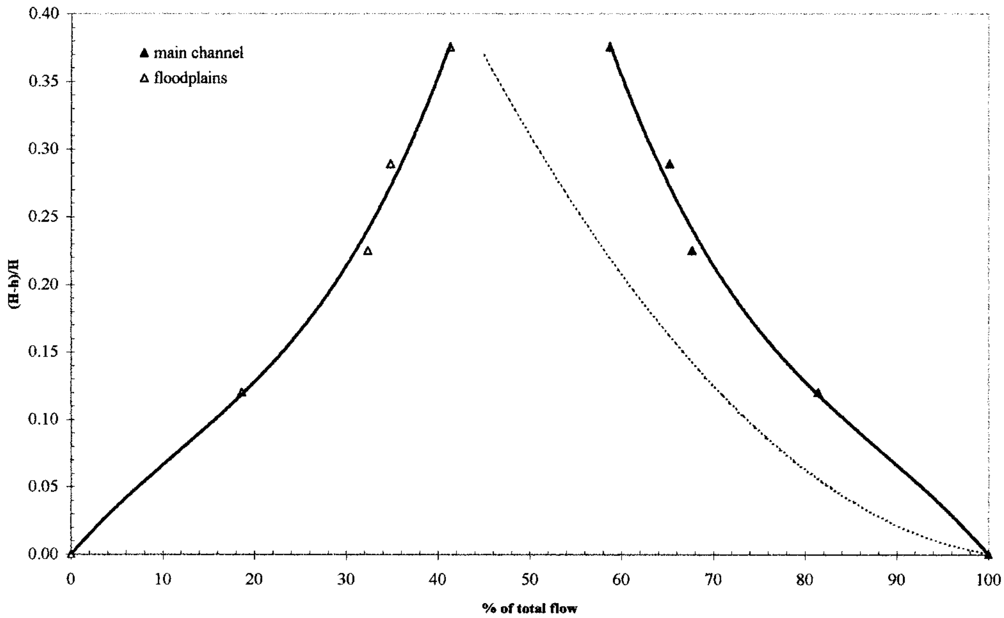

Fig. 13. Percentage of total flow in main channel, $\%Q_{mc}$, rough floodplains, and $\%A_{mc}$

bankfull to a value of 0.0231 just above bankfull, a reduction of 73%. Similarly the Manning coefficient drops from a value of 0.0246 to a value of 0.0102, a reduction of 59%. This apparent reduction is caused solely by the abrupt change in hydraulic radius as the flow goes overbank. Using the Manning formula to calculate the resistance as the flow goes just overbank, with the area, discharge and slope remaining constant, the following relationship is obtained:

$$\frac{n_{overbank}}{n_{bankfull}} = \frac{S^{1/2} R^{2/3}_{overbank} A/Q}{S^{1/2} R^{2/3}_{bankfull} A/Q} = \frac{R^{2/3}_{overbank}}{R^{2/3}_{bankfull}} \tag{4}$$

Hence a decrease in resistance of 59% is given by a decrease in hydraulic radius of 74%. In these experiments the hydraulic radius changed abruptly from a bankfull value of 0.1654m to a value of 0.0441m just above bankfull, on account of the 6.0m of additional wetted perimeter being added to P without any additional increase in area, A. This serves to illustrate why the hydraulic radius (R=A/P) is such a poor channel parameter to use for resistance studies in overbank flow, unless properly understood and applied. See Myers & Brennan (1990) and Myers, Knight, Lyness, Cassells (1998), Cassells & Brown (1999).

Above bankfull the overbank smooth data initially increase, reaching a maximum at a depth of around 0.28m, and then show a slight decrease. This is due to the smooth floodplains becoming a greater proportion of the channel conveyance area as the depth increases. The overbank rough floodplain data on the other hand show an almost linear and continuous increase with depth, on

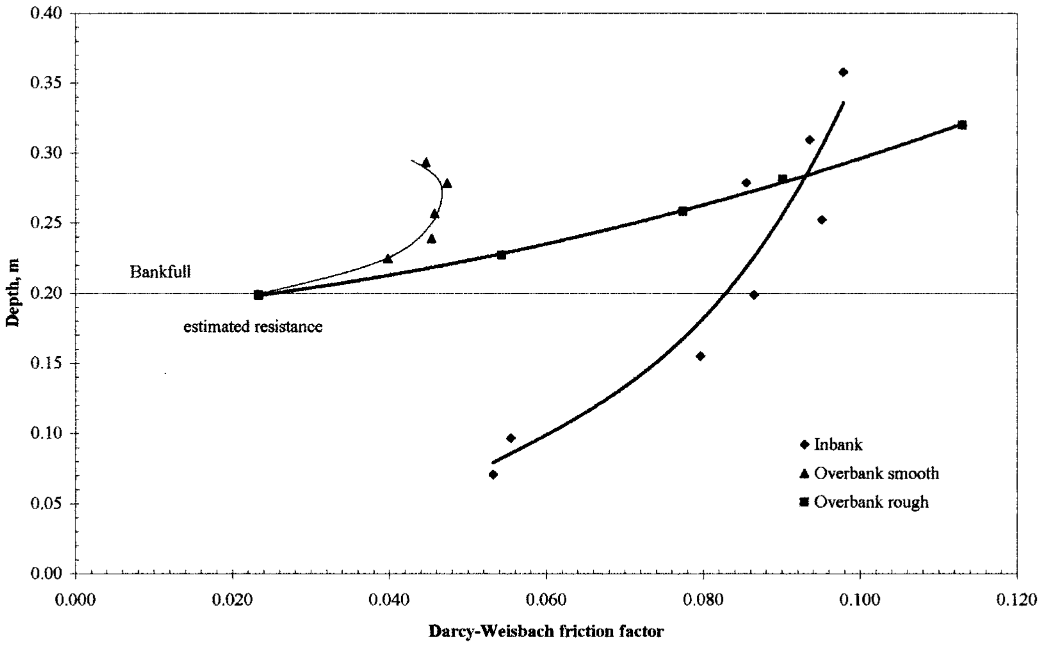

Fig. 14. Overall values of Darcy-Weisbach friction factor, f v H

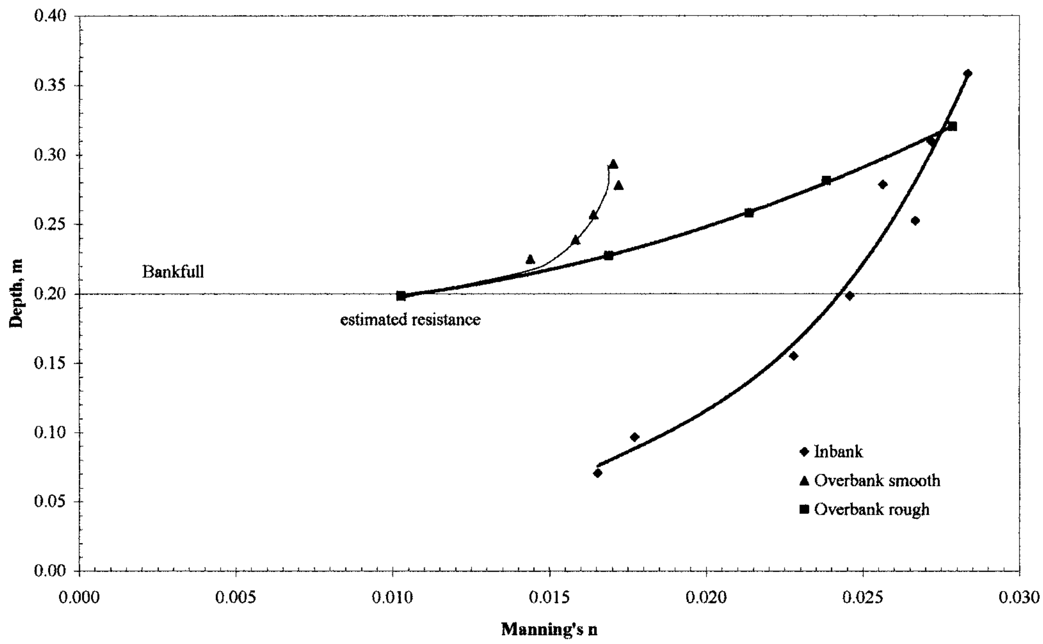

Fig. 15. Overall values of Manning's resistance coefficient, n v H

account of the drag force on the dowel rods (roughness elements) increasing as the floodplain velocity increases and because more of each dowel is in contact with the flowing water.

The variation of f with Reynolds number is shown in Fig. 16, along with the smooth law of Prandtl. The 'overbank smooth' values are approximately constant, but much higher than the Prandtl smooth law curve, due to the influence of the main channel bedforms. Comparison of the overbank smooth data with a Moody diagram would put the channel in the rough turbulent zone with a relative roughness, $k_s/4R$, of approximately 0.020. The 'overbank rough' and 'inbank' data both increase with Reynolds number, due to increasing bedform roughness and floodplain roughness.

In order to understand these data and the influence of the mobile bed on overbank flows, a comparison was made with some rigid boundary compound channel resistance data from Phase A (See Knight, 1992). Fig. 17 shows some FCF Phase A data reproduced from Shiono & Knight (1991), obtained from an earlier series of experiments with different floodplain widths (B/b ratios). In these earlier experiments, the main channel base width was 1.5m, the side slopes were 1:1, and the bankfull depth, h, was 0.15m, giving a main channel aspect ratio of 10 and B/b values of 6.67, 4.2 & 2.2. This compares with an aspect ratio value of 8 (= 1.6/0.2) in the present series of loose boundary experiments, and a B/b value

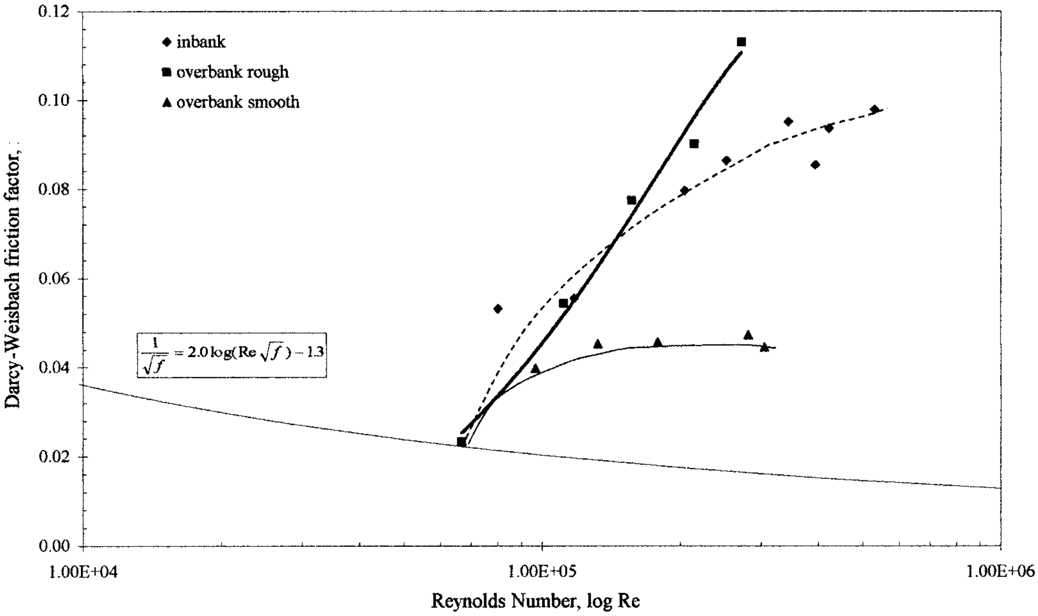

Fig. 16. Variation of the overall Darcy-Weisbach friction factor, f v Re, FCF Phase C

of 5 (= 4.0/0.8). Thus although the geometry was not identical, it was similar enough to make comparisons.

Fig. 17 shows how for a rigid boundary compound channel, as the flow increases for a particular B/b ratio, the inbank f values (marked as x in Fig. 17 for B/b=1.2) initially follow the Prandtl smooth law, and decrease with increasing Reynolds number. At the bankfull stage there is the characteristic discontinuity, arising from an abrupt change in hydraulic radius, R. The overall f value then jumps to a much lower value, as does the Reynolds number, in an analogous way to the discontinuity in the f v depth relationship already shown in Fig. 14. As the overbank flow increases, the overall f values for a particular B/b ratio then increase with increasing floodplain depth, and come back towards the Prandtl law as the channel becomes more amenable to being treated as a single channel. The f v Re relationship is therefore complex, even for rigid boundary channels, and very different from the conventional Moody diagram based on the Colebrook-White equation.

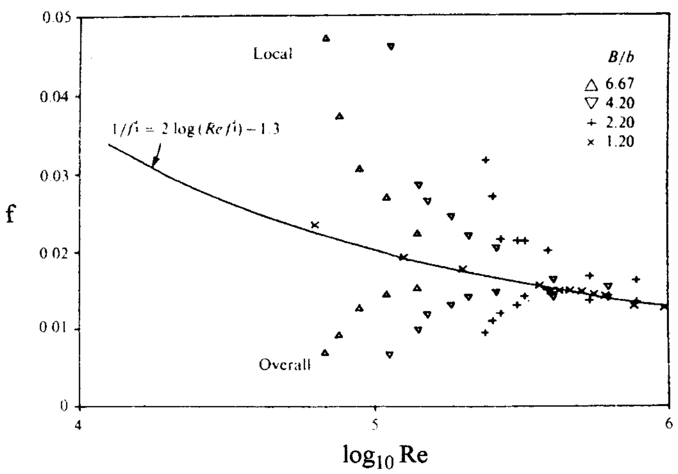

Fig. 17. Variation of the overall Darcy-Weisbach friction factor, f v Re, FCF Phase A

For loose boundary channels, the overall resistance coefficients shown in Fig. 16 are clearly much larger than those in Fig. 17, lie above the smooth law, and the overbank data do not quite follow the same trend as the rigid boundary results. Also shown in Fig. 17 are the laterally averaged local floodplain resistance coefficients, f_b, (based on Eq. (5) described shortly) which are seen to be much larger than the overall resistance coefficients. The 'local' values form a herring bone pattern for different B/b ratios on the opposite side of the Prandtl smooth law to the 'overall' values. At low submergence on the floodplains the local values are 4 to 5 times larger than the overall values. In order to understand the difference between overall, zonal and local resistance coefficients, the data were examined in further detail.

3.2 Main channel and floodplain zonal resistance coefficients

Using the discharges presented in Figs 12 & 13, the 'zonal' resistance coefficients for the main channel and the floodplains were evaluated by dividing the channel into sub areas, using a vertical interface at each bankfull channel edge, and values are given in Table 3 for each test. The length of the interface was excluded from the calculation of wetted perimeter for each zone, and no account was taken of any shear forces that might be present along these interfaces arising from lateral momentum transfer. The procedure for calculating these resistance coefficients was thus based on one of the simple 'divided channel' methods (Myers & Brennan, 1990; Myers et al. 1997).

Figs 18 & 19 show the zonal Manning n values for smooth and roughened floodplain cases, together with the overall n values, based on the single channel method, taken from Fig. 15. Similar plots are obtained if values of f are used instead of n (Brown 1997). Fig. 18 shows that when the floodplains are smooth, the overbank resistance values, labelled 'divided channel-flood plain (Δ), are low at around 0.010, much less than the main channel values, which range from around 0.025 to 0.033. These zonal val-

Table 3. Summary of overall and zonal resistance coefficients

Test No	Layout	Q m^3s^{-1}	H mm	Overall n	Zonal n main channel	Zonal n floodplains
131195	inbank	0.050	0.071	0.01654	0.01654	-
260695	"	0.075	0.097	0.01772	0.01772	-
030795	"	0.125	0.155	0.02279	0.02279	-
100795	"	0.175	0.199	0.02459	0.02459	-
201195	"	0.250	0.253	0.02667	0.02667	-
260396	"	0.300	0.279	0.02563	0.02563	-
221195	"	0.350	0.310	0.02720	0.02720	-
271195	"	0.450	0.358	0.02836	0.02836	-
estimate	rough	0.175	0.199	0.01026	-	-
160795	"	0.250	0.227	0.01690	0.02899	0.01369
240795	"	0.350	0.258	0.02138	0.03083	0.01942
310795	"	0.450	0.281	0.02385	0.02972	0.02517
080895	"	0.600	0.320	0.02788	0.03119	0.03035
estimate	smooth	0.175	0.199	0.01026	-	-
140496	"	0.250	0.225	0.01439	0.02648	0.00924
140895	"	0.350	0.239	0.01583	0.03059	0.00879
290895	"	0.450	0.257	0.01640	0.03150	0.00975
210895	"	0.600	0.278	0.01721	0.03295	0.01089
170496	"	0.750	0.293	0.01703	0.03410	0.01084

ues, based on the 'divided channel' method of computation, are naturally either side of the overall values (◊), based on treating the channel as a single unit, shown with a solid line around 0.015. In reality the floodplain resistance may be greater than that shown here on account of the shearing force which may be present on the interface, but excluded in this simple analysis. These zonal values are important, since they are frequently used in the divided channel method to give the correct discharge in each sub area. The corresponding overbank 'divided channel-flood plain' zonal resistance values for rough floodplains, shown in Fig. 19, are seen to increase much more rapidly with depth than the smooth values, due to the dowel rods.

Figs 18 & 19 also serve to illustrate the difficulty of combining 'roughness' coefficients for a heterogeneously roughened channel, with a compound shape, into a single composite 'resistance' value (Chow, 1959; Yen, 1992). The importance of applying cor-

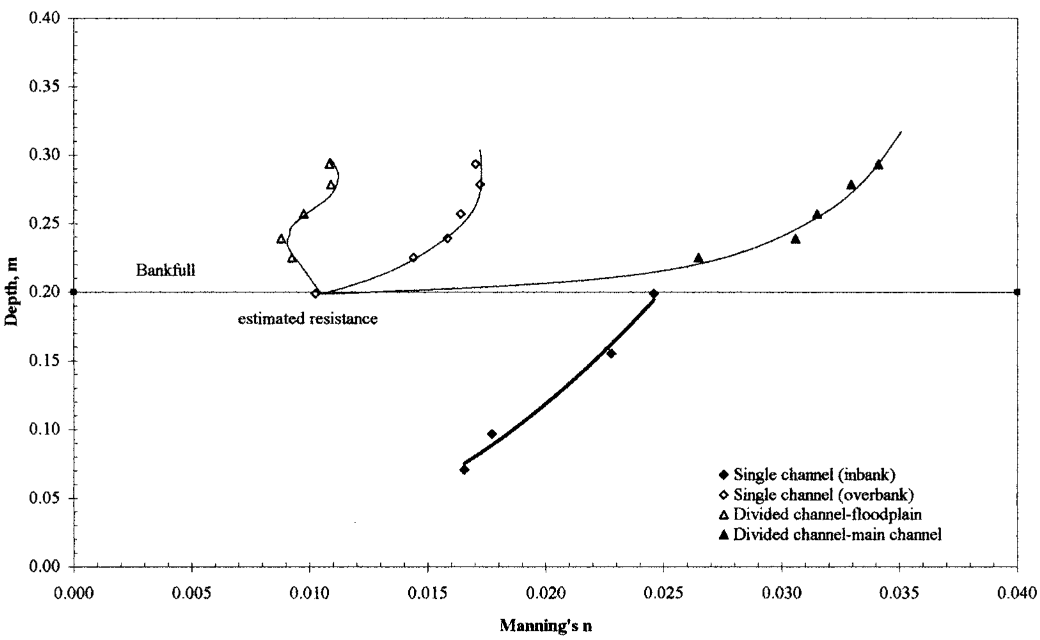

Fig. 18. Comparison of Manning resistance coefficients by divided and single channel methods, smooth floodplains

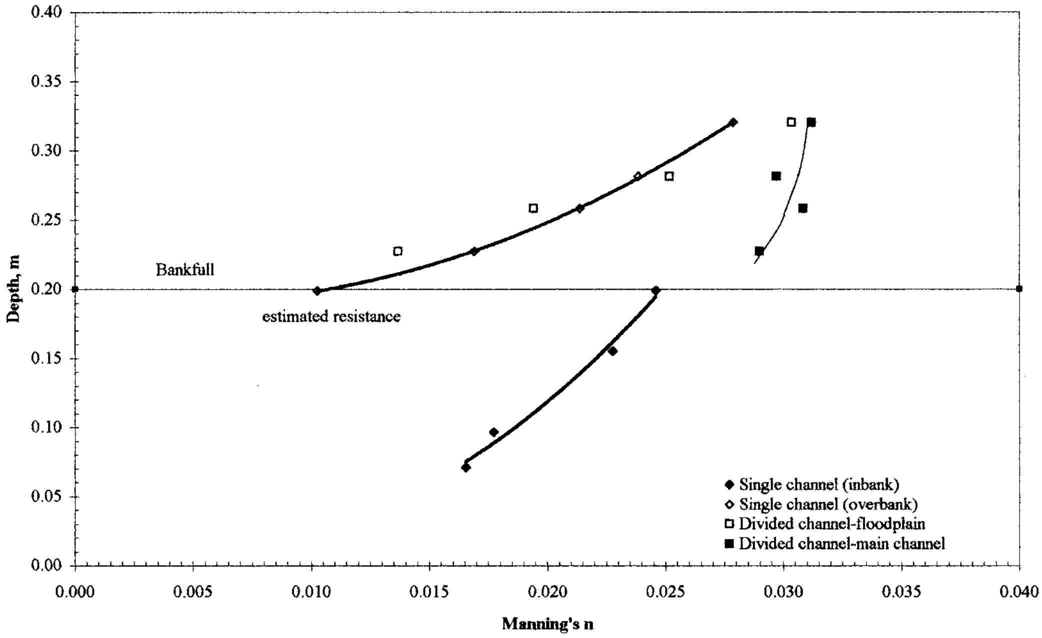

Fig. 19. Comparison of Manning resistance coefficients by divided and single channel methods, rough floodplains

rect 'zonal' or 'overall' resistance coefficients are illustrated with respect to a natural river by Knight, Shiono & Pirt (1989), based on field measurements over a range of overbank flows. Technically it is better to use individual 'roughness' coefficients appropriate to the textural properties of each boundary surface, rather than 'resistance' coefficients as used here Adjustments should then be made to the zonal discharges at a later stage. This is the method adopted by Ackers (1992 & 1993a&b) in the 'coherence' method of calculation for compound channels. Fig. 20 shows all the zonal resistance coefficients, taken from Figs 15, 18 & 19, plotted together for the purposes of comparison.

3.3 Local resistance coefficients

Local resistance coefficients were obtained from combined measurements of local boundary shear stress and depth-averaged velocity across each floodplain. Fig. 21 shows a typical set of boundary shear stress measurements, made using a Preston tube, for a discharge of 0.6 m^3s^{-1}, over smooth floodplains. The data are seen to be reasonably symmetric and the average boundary shear stress on each floodplain was much the same. Combining such data with the corresponding depth-averaged velocity data, gives the lateral variation of the local resistance coefficient, f_b, expressed by

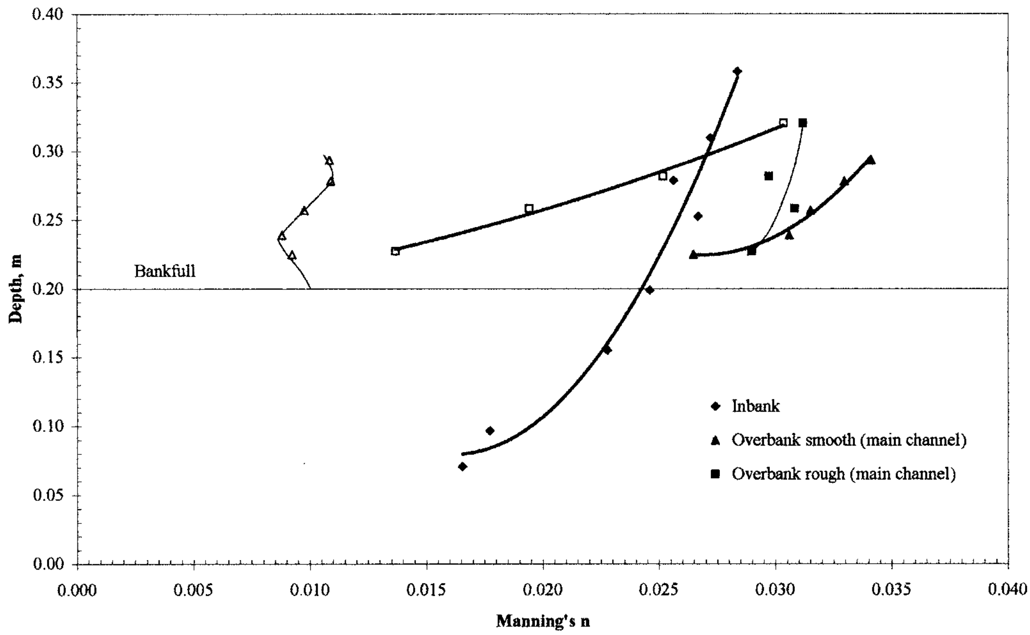

Fig. 20. Zonal values of Manning resistance coefficients by divided and single channel methods

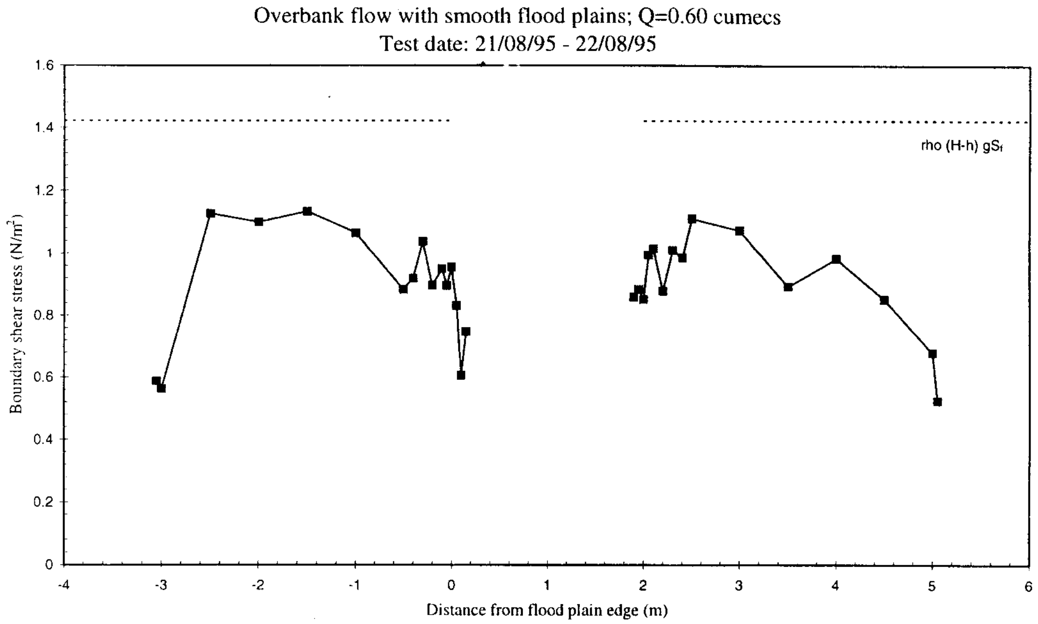

Fig. 21. Boundary shear stress measurements, 210895, Q = 0.60 m^3s^{-1}, smooth floodplains

$$\tau_b = \left(\frac{f_b}{8}\right)\rho U_d^2 \tag{5}$$

where U_d is the depth averaged velocity defined generally by

$$U_d = \frac{1}{H}\int_0^H U dz \tag{6}$$

and f_b is the local resistance coefficient. On the floodplain, H in Eq. (6) is replaced by the local depth (H-h).

Fig 22 shows one set of results, based on the velocity and boundary shear stress data presented in Figs 11 & 21 for a discharge of 0.6 m^3s^{-1}. The lateral distributions of the local f values across each floodplain are seen to be uniform, giving a laterally averaged value of around 0.015, well below the two-dimensional value of 0.022, shown by the dotted line and given by the expression based on local depth

$$\tau = \rho g\,(H\text{-}h)\,S_f \tag{7}$$

Because the velocity and boundary shear stress tend towards uniform values, especially for wide floodplains, they are often treated as zonal values equivalent to a 'wide' channel. Although commonly done, this still masks the influence of secondary flows and temporal averaging of the turbulent eddies on the floodplain (Knight & Shiono, 1996, Wormleaton, 1996). Ignoring these effects, the difference between the local and the two-dimensional

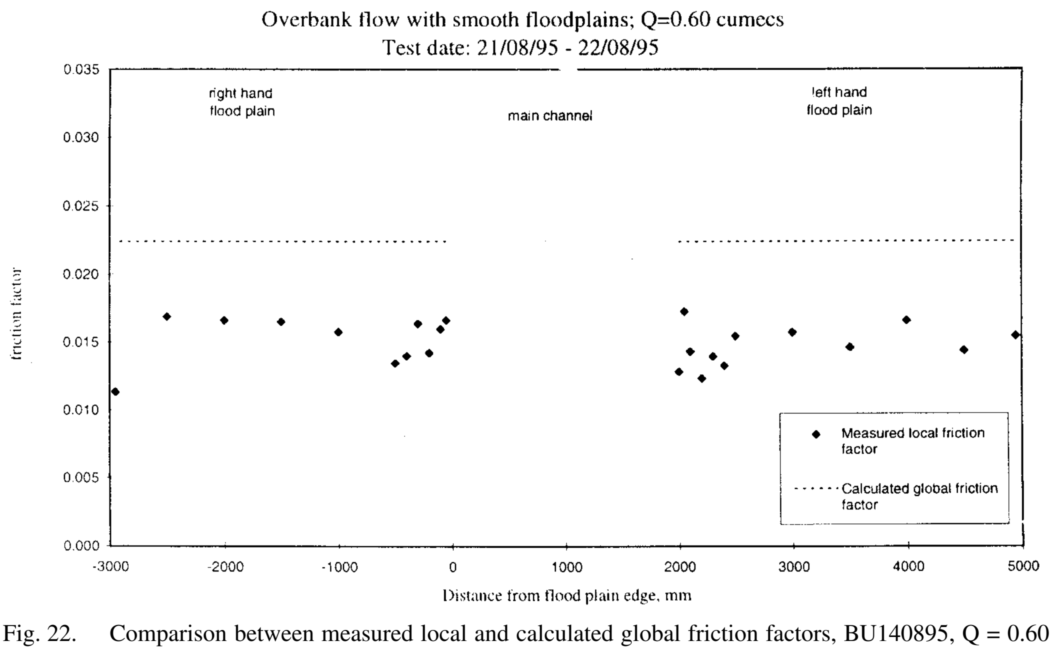

Fig. 22. Comparison between measured local and calculated global friction factors, BU140895, Q = 0.60 m^3s^{-1}

(zonal) value is usually expressed by

$$\tau_b = K\rho g\,(H-h)\,S_f \tag{8}$$

where K is a factor to account for the turbulent eddies. Values of K were calculated from the measured data and the smooth floodplain results are shown in Fig. 23. It is clear that for a relative depth, Dr, greater than 0.19, where Dr = (H-h)/H, the factor K is less than 1.0, implying that the local shear stress values are lower than those calculated by Eq. (7). Simple exponential equations based on the relative depth, Dr, were fitted through the data, and the smooth floodplain results gave

$$K_{fp} = 0.193 Dr^{-0.991} \tag{9}$$

Equations (5), (8) & (9) thus link the local resistance coefficient and velocity with the local shear stress for this particular case, and indicate how the local shear stress differs from the overall shear stress ($\tau = \rho gRS_f$). Further analysis and details of these K factors for compound channels are given in Knight & Shiono (1996) and Abril & Knight (2000).

3.4 Alluvial bed resistance coefficients

In order to obtain the bed resistance coefficients for all inbank flows, it was necessary to subtract the influence of the two smooth sidewalls from the main channel or zonal resistance coefficients. This was achieved by using four standard sidewall correction procedures, Pavlovskii, Krishnamurthy & Christensen, Lotter and the shear force balance method (see Chow, 1959; Yen, 1992), and assessing their merits against the boundary shear stress values actually measured along the sidewalls. The four methods gave very similar results, as shown by Fig. 24. The results were then combined and the equation of linear best fit for the bed resistance was found as follows:

$$n = 0.0612\,H + 0.0133 \tag{10}$$

The mean bed shear force, and hence mean boundary shear stress, acting on the 1.6m wide sand bed of the alluvial main channel could then be calculated for any depth of flow, H.

Any sidewall correction procedure effectively reduces the main channel to an equivalent 'wide' channel, and allows for the effect of channel shape (aspect ratio), and heterogeneous roughness distribution. In the case of inbank flows, and embanked main channel flows with sidewalls, the procedure is directly applicable. However for overbank flows in compound channels, the additional shear stresses due to the main channel/floodplain interaction need to be accounted for in the overall force balance, prior to determining the component bed shear stress. In the case of smooth floodplains, the lateral distribution of velocity shown in Fig. 11 indicates that this interaction, and hence shear stress, was very small. Under these circumstances the sidewall procedure might be justified for this particular case, although not used here, since more advanced methods are available (Knight, Yuen & Alhamid, 1994).

Having obtained the correct resistance coefficients for the bedforms, they could be compared with those obtained from standard fluvial resistance formulae, such as those by White, Paris & Bettess (1980) and van Rijn (1984). Fig. 25 shows these comparisons for the inbank flow data only, over a range of discharges, expressed in terms of a discrepancy ratio (calculated resistance/observed resistance).

4. Discussion of results

4.1 Stage discharge relationships

The basic H v Q curves shown in Fig. 9 are reasonably well represented by the second order relationships of Eq. 1. As would be expected, for a given stage, the total channel discharge, Q_{total}, is

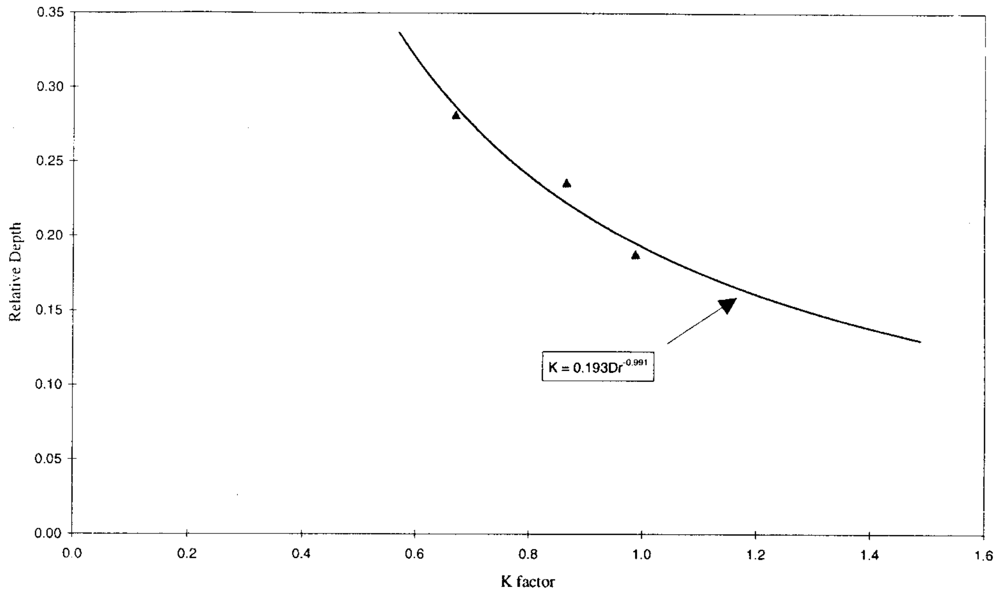

Fig. 23. Discrepancy between measured and calculated local shear stresses on floodplains: the K factors required in Equation (8)

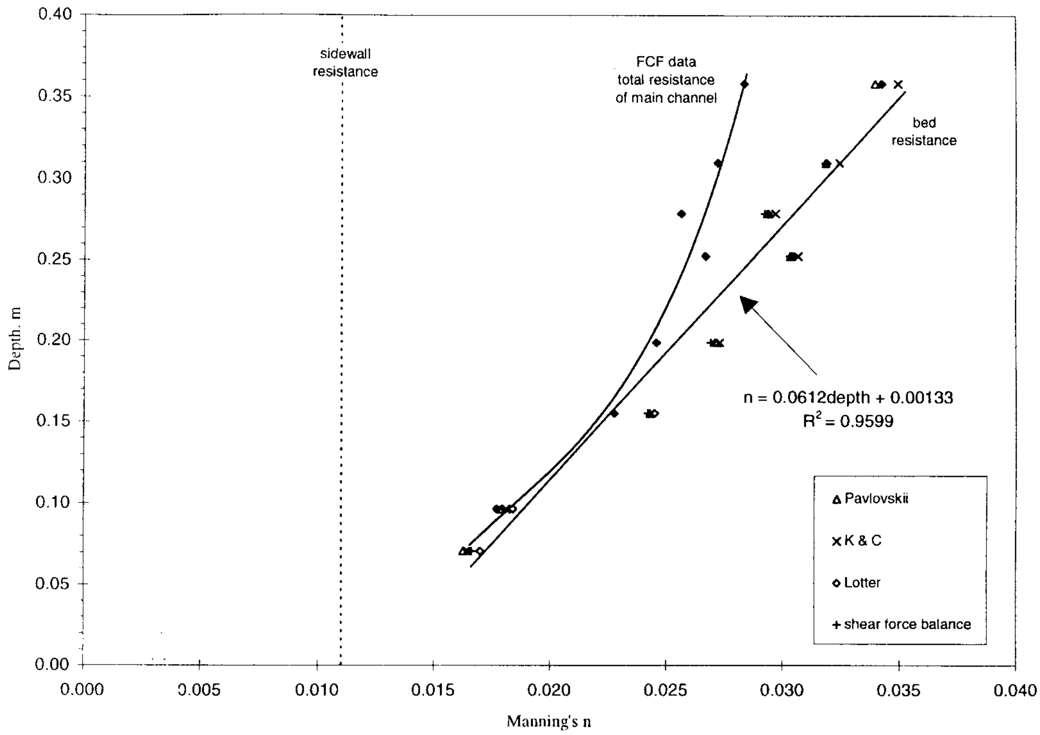

Fig. 24. Comparison of sidewall correction formulae applied to main channel

largest when overbank flow occurs with smooth floodplains. However, when the stage is plotted against the main channel discharge, Q_{mc}, as shown in Fig. 26, it is clear that the conveyance capacity of the main channel is surprisingly greater when the floodplains are rough rather than smooth. Also shown in Fig. 26 are the single channel data taken from Fig. 9 for ease of comparison.

It is clear that the prediction of the stage discharge relationship for a mobile bed channel with floodplains is a complex issue. Not only does the shape of the cross section change markedly at the bankfull stage, but also the different roughnesses have to be combined into zonal resistance values to obtain the correct discharge in each sub area. For practical reasons it is important that these zonal discharges are determined accurately as they influence other engineering calculations concerning zonal resistance, boundary shear stress and sediment transport. Figs 12 & 13 show that these zonal discharges are very different from the area percentage values, and also considerably different from the rigid boundary data of Phase A (Knight, 1992).

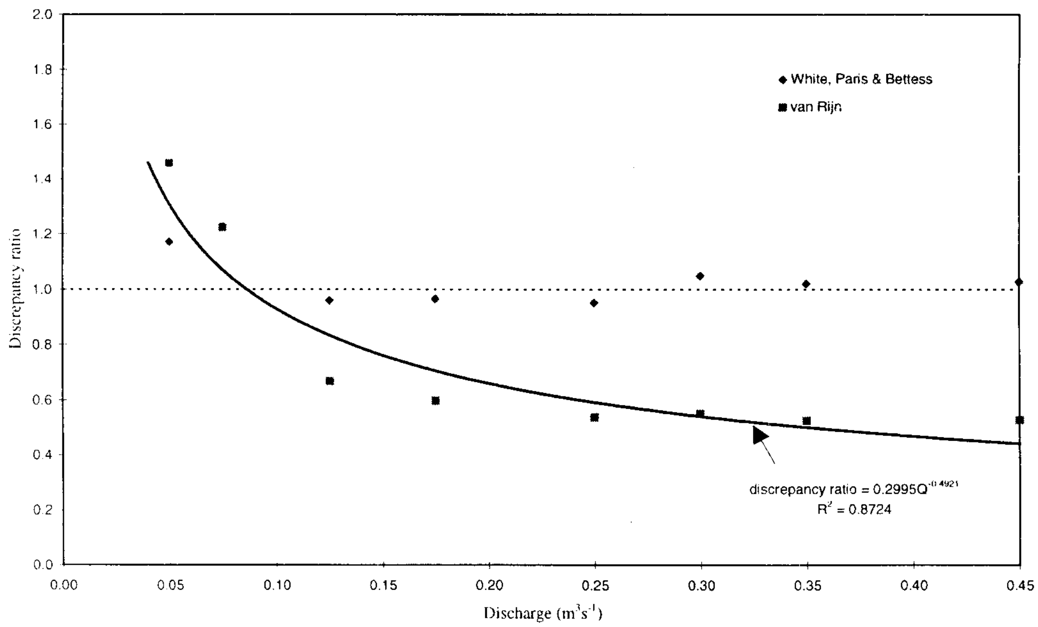

Fig. 25. Discrepancy between observed and calculated alluvial bed resistance coefficients

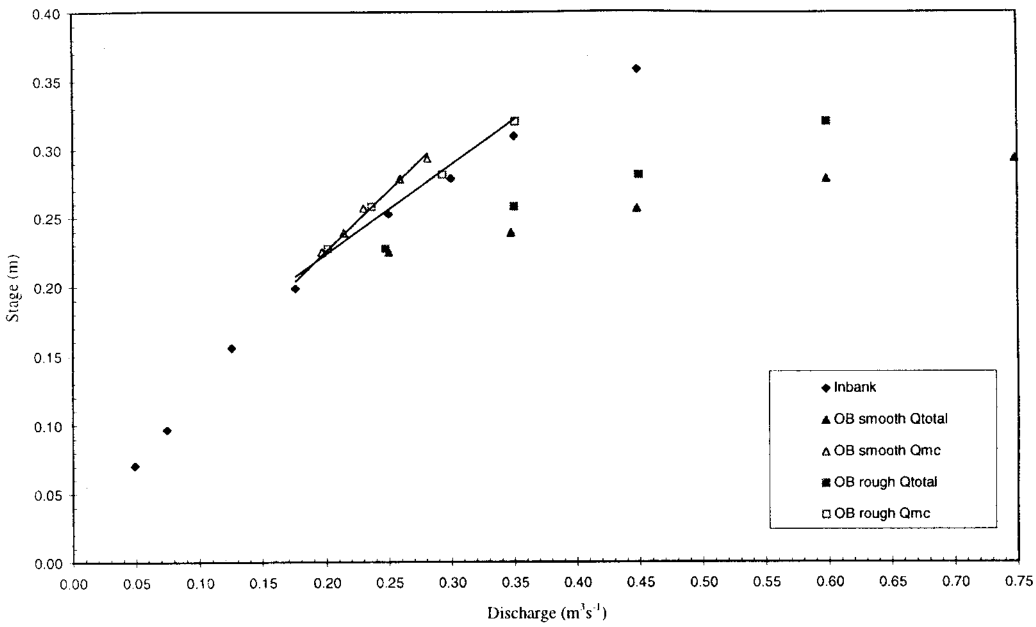

Fig. 26. Stage discharge data, showing both total and main channel discharges

4.2 Overall, zonal and local resistance coefficients

Resistance coefficients are important because the *overall* values give the stage-discharge relationship for the whole cross section, the *zonal* values give the correct discharge in any sub region, and the *local* values give the local boundary shear stress in terms of the local depth-averaged velocity. The local values are particularly important because the boundary shear stress, τ_o, or shear velocity, u*, ($= \sqrt{\{\tau_o/\rho\}}$) occurs in many other hydraulic equations related to sediment and pollutant transport. The cross section average boundary shear stress may be derived for uniform flow by balancing the gravitational force down the channel ($= \rho g A S_f$) with the retarding force at the channel boundaries ($= \tau_o P$) to give

$$\tau_o = \rho g R S_f \tag{11}$$

The mean boundary shear stress is then traditionally linked to the section mean velocity, U_A, by dimensional arguments, to define a mean or overall friction factor, f_o, as

$$\tau_o = \left(\frac{f_o}{8}\right)\rho U_A^2 \tag{12}$$

Equations (11) & (12) are in fact the basis of the Darcy-Weisbach resistance law, given as Eq. (3). For very wide channels (b/h > 20 for < 5% error) then the local depth, H, may be used instead of the hydraulic radius, R, to give an approximate value for the mean boundary shear stress,

$$\tau_o \approx \rho g H S_f \tag{13}$$

which was the form adopted in Eq. (7) when dealing with the local floodplain values.

The relationship between local boundary shear stress and the cross section average is difficult to determine theoretically, even for simple channel shapes (Knight, Yuen & Alhamid, 1994). Eqs (5) & (12) show that care needs to be taken to distinguish between the depth-averaged velocity, U_d, and the section-mean velocity, U_A, as well as between the local depth, H, and the hydraulic radius, R. It is also very important to distinguish between overall, zonal and local friction factors, f_o, f_b and f. The zonal resistance coefficient is one that relates streamwise weight force with boundary shear force, including implicitly other shear forces that might be acting on the element sides due to lateral shear or secondary flows. The local resistance coefficient is the zonal value, taken to the limit, with an extremely small element width in the lateral direction. The overall and zonal resistance coefficients are therefore linked to the method of analysis adopted, in this case the 'single' and 'divided' channel approaches.

Comparison of the overall and zonal resistance coefficients for the smooth floodplain data in Fig. 18, shows that the resistance of the main channel by the divided channel method is approximately double that of the entire channel based on the single channel method. The resistance of the floodplain is approximately 40% smaller than that of the entire channel based on the single channel method. With roughened floodplains, Fig. 19 shows that the resistance of the main channel is almost constant with depth. Hence at low floodplain depths the resistance is considerably greater than that given by the single section method, but as the depth increases the single and divided section resistance values tend to equalise. For the same depth, the zonal roughness of the main channel appears to be greater if the floodplains are smooth than if the floodplains are rough, as shown in Fig. 20, which compares data from Figs 18 & 19. This is a surprising result since the bedforms are known to be similar. It must therefore be due to some other influence, perhaps secondary flow, at the main channel/floodplain interface. The zonal resistance data in Fig. 20 is, of course, linked directly to the zonal stage discharge data presented in Fig. 26.

4.3 Alluvial channel resistance coefficients

Fig. 25 shows a small part of the very detailed analysis which has been undertaken on these data in order to obtain alluvial bed resistance coefficients. All the results lie well within a factor of two of the observed values. The WPB formula gives a consistently more accurate prediction than the van Rijn formula, with a mean discrepancy ratio of 1.047, and a standard deviation of 0.101, giving a mean error of 4.72% ±10.13%. Further analysis of the boundary shear stress and bedform data, and the grain/form roughness and alluvial friction, are in progress.

The difficulty in obtaining high quality data from alluvial channels with overbank flow has been highlighted by these experiments. Even under strict laboratory conditions, as with the FCF, there is considerable temporal variability in water surface slope and significant spatial variability in the longitudinal bed profiles. Taken together with the complex cross sectional shape, the interaction between the main channel and its floodplains, and the heterogeneous roughness distribution, makes accurate measurement of the primary hydraulic parameters exceedingly difficult. Field data, although highly desirable, requires comprehensive spatial data that are clearly an order of magnitude more costly and difficult to obtain, especially so given the dynamic nature of natural flood events. Experiments such as those outlined in this paper are therefore seen to be justified, as being potentially one of the only sources of detailed information on these types of channel flow. However, it must be recognised that even at this so called 'large scale', scale effects are still a problem and need clarifying further.

4.4 Modelling strategies for two stage channels with sediment

Various attempts at modelling sediment transport with overbank flows have been made using different approaches based on the divided channel method, the coherence method and the Shiono & Knight method (Abril and Knight, 2002; Ackers, 1992; Ayyoubzadeh, 1997; Knight and Shiono, 1996; Knight and Abril, 1996). Details of the very extensive finite element modelling are given in Abril (1997). All methods have some difficulty in representing the correct H v Q relationship, the proportion of flow in any given sub-area, the boundary shear stress distribution and the sediment transport rate, let alone bedform structure. It is not surprising therefore that there is no consensus on the most appropriate strategy for modelling two-stage channels with sediment.

5. Conclusions

1. Recent experiments conducted in the UK Flood Channel Facility (FCF) have been described. Some experimental data on overbank flows with alluvial sand channels for one type of geometry, bed slope and sand size have been analysed and presented.
2. The size of bedforms and their effect on the temporal variation of water surface profiles, bed profiles, sediment transport rate and cross sectional shape have been illustrated through a series of photographs and diagrams in Figs 1 - 8.
3. Stage-discharge data have been presented in Tables 1 - 3 and Figs 9 & 26, for both inbank and overbank flows, and two types of floodplain roughness.
4. The proportion of the total discharge occurring in the main river channel, $\%Q_{mc}$, is shown in Figs 12 & 13 to be different from the corresponding proportion of the main channel area, expressed as a percentage of the total area. The variation of these proportions with depth is also significantly different from previous rigid boundary results, obtained in Phase A of the FCF programme.
5. The difference between overall, zonal and local resistance coefficients has been highlighted through equations (5) & (12) and in Figs 14-20. The variation of the main channel (zonal) resistance coefficient is shown to vary threefold, due to the size of the bedforms changing with flow conditions and depth.
6. Figs 14 & 15 show how the Darcy-Weisbach and the Manning overall resistance coefficients drop 73% & 59% respectively just above bankfull stage, arising from abrupt changes in hydraulic radius. Figs 16 & 17 show the effect of this discontinuity on the f v Re and depth v Manning coefficients relationships. Due to the variation of main channel resistance with stage, these relationships differ from the corresponding relationships for rigid boundary compound channels.
7. Figs 18 - 20 show how the smooth floodplain zonal resistance coefficients initially increase, and then reach a local maximum for overbank flow, whereas the roughened floodplain coefficients increase continuously with overbank depth, due to the increased drag force on the dowels and the greater length in contact with the water.
8. Lateral distributions of velocity and boundary shear stress on the floodplains were used to calculate the lateral variation of local friction factor. Typical data are shown in Figs 11, 21 & 22 for one particular discharge. The difference between the local and the two-dimensional resistance coefficients, via an adjustment factor K based on equation (8), is shown in Fig 23 for a range of depths over smooth floodplains. These data illustrate the discrepancies that can arise by calculating the local boundary shear stresses from the local depth and energy gradient.
9. The size of the main channel bedforms, relative to the bankfull height, the type of floodplain roughnesses adopted for these experiments, the range of flows tested and the large scale of the FCF, mean that these data provide particularly challenging cases for the river engineering analyst to numerically model. For example, in the case of roughened floodplains, three types of boundary roughness apply to different elements of the wetted perimeter, two of which vary with discharge, and these need to be composited together in order to obtain a prediction for the stage discharge relationship.
10. Further careful experimentation at various scales is required, on account of the inevitable limitations of these FCF data and the paucity of field data. It is essential that the component physical processes be understood better, and that further laboratory data for a wider range of sediments, channel shapes and flow conditions be obtained.

Acknowledgements

The authors would like to express their gratitude to the EPSRC for their sustained funding for the FCF programme of research, without which these data could not have been obtained. Particular thanks are also due to their colleagues from the universities of Newcastle and Ulster, without whose assistance, dedication and team approach, the data would not have been possible to obtain. They would also like to thank Dr Roger Bettess, and the technical staff at HR Wallingford, whose assistance and support made the work on the FCF possible.

Notation

A area
b semi-breadth of main channel
B semi-breadth of channel to floodplain boundaries
d sediment size
Dr relative depth { = (H-h)/H }
f Darcy-Weisbach resistance coefficient (general)
f_b local friction factor
f_o overall friction factor
Fr Froude number
g gravitational acceleration
h bankfull depth (nominally 200 mm)
H depth of flow in main channel
K coefficient, used in Eq. (8)
K_{fp} coefficient, used in Eq. (9)
n Manning resistance coefficient ($m^{-1/3}$ s)
P wetted perimeter
Q discharge
R hydraulic radius (= A/P)
Re Reynolds number (= 4UR/ν)
S bed slope
S_f friction or energy slope
U velocity
U_A section mean velocity (= Q/A)
U_d depth averaged velocity
k_s Nikuradse equivalent sand roughness size
ρ fluid density
τ boundary shear stress
ν kinematic viscosity

References

Abril, B., and Knight, D.W., 2002, "Stage-discharge relationships for rivers in flood: Theory & Application", *Journal of Hydraulic Engineering*, ASCE, (submitted for publication).

Abril, B., 1997, "Numerical river modelling of turbulent flow, sediment transport and flood routing using the finite element method", *PhD thesis*, The University of Birmingham, England, UK.

Ackers, P., 1992, "1992 Gerald Lacey Memorial Lecture - Canal and river regime in theory and practice : 1929-92", *Proc. Instn Civ. Engrs Wat., Marit. & Energy,* 96, Sept., Paper No. 10019, pp 167-178.

Ackers, P., 1992, "Hydraulic design of two stage channels", *Proc. Instn Civ. Engrs Wat., Marit. & Energy,* 96, Dec., Paper No. 9988, pp 247-257.

Ackers, P., 1993a, "Stage -discharge functions for two-stage channels : The impact of new research", *Journal Instn Water & Environmental Management,* Vol. 7, No. 1, February, pp 52-61.

Ackers, P., 1993b, "Flow formulae for straight two-stage channels", *Journal of Hydraulic Research,* IAHR, Vol. 31, No. 4, pp 509-531.

Atabay, S. and Knight, D.W., 1999, "Stage discharge and resistance relationships for laboratory alluvial channels with overbank flow", In River Sedimentation [Eds A W Jayawardena, J H W Lee & Z Y Wang], *Proc. Seventh International Symposium on River Sedimentation, Hong Kong, December 1998*, pp 223-229.

Ayyoubzadeh, S.A., 1997, "Hydraulic aspects of straight-compound channel flow and bedload sediment transport", PhD thesis, The University of Birmingham, England, UK.

Brown, F.A., 1997, "Sediment transport in river channels at high stage", PhD thesis, The University of Birmingham, England, UK.

Cassells, J., 1998, "Hydraulic characteristics of straight mobile bed compound channels with uniform sediment", PhD thesis, University of Ulster.

Chow, V.T., 1959. "Open Channel Hydraulics", McGraw-Hill, New York.

Knight, D.W., 1981, "Some field measurements concerned with the behaviour of resistance coefficients in a tidal channel", *Estuarine, Coastal and Shelf Science*, Academic Press, London, No. 12, pp 303-322.

Knight, D.W. and Demetriou, J.D., 1983, "Flood plain and main channel flow interaction", *Journal of Hydraulic Engineering,* ASCE, Vol. 109, No. 8, August, pp 1073-1092.

Knight, D.W., and Sellin, R.H.J., 1987, "The SERC Flood Channel Facility", *Journal of the Institution of Water & Environmental Management,* Vol. 1, No. 2, October, pp 198-204.

Knight, D.W., Shiono, K. and Pirt, J., 1989, "Prediction of depth mean velocity and discharge in natural rivers with overbank flow", *Proc. Int. Conf. on Hydraulic and Environmental Modelling of Coastal, Estuarine and River Waters*, (Ed. R.A. Falconer, P. Goodwin, R.G.S. Matthew), Gower Technical, University of Bradford, September, Paper 38, pp 419-428.

Knight, D.W. and Shiono, K., 1990, "Turbulence measurements in a shear layer region of a compound channel", *Journal of Hydraulic Research,* IAHR, Vol. 28, No. 2, 1990, pp 175-196, (Discussion in IAHR Journal, 1991, Vol. 29, No. 2, pp 259-276).

Knight, D.W. [Ed], 1992, "SERC Flood Channel Facility experimental data - Phase A", Vols 1-15, SR Report No. 314, HR Wallingford, (available from HR Wallingford, Oxon, OX10 8BA, UK).

Knight, D.W., Yuen, K.W.H. and Alhamid, A.A.I., 1994, "Boundary shear stress distributions in open channel flow", in *Physical Mechanisms of Mixing and Transport in the Environment,* (Ed. K. Beven, P. Chatwin & J. Millbank), J. Wiley,

Chapter 4, pp 51-87.
KNIGHT, D.W., and ABRIL, B., 1996, ''Refined calibration of a depth averaged model for turbulent flow in a compound channel'', *Proc. Instn of Civil Engineers, Water, Maritime and Energy*, Paper 11017, Vol. 118, Sept., pp 151-159.
KNIGHT, D.W. and SHIONO, K., 1996, ''River channel and floodplain hydraulics'', In *Floodplain Processes*, [Eds Anderson, Walling & Bates], Chapter 5, J. Wiley, pp 139-181.
KNIGHT, D.W., BROWN, F.A., AYYOUBZADEH, S.A., & ATABAY, S., 1999, ''Sediment transport in river models with overbank flow'', In River Sedimentation [Eds A W Jayawardena, J H W Lee & Z Y Wang], *Proc. Seventh International Symposium on River Sedimentation, Hong Kong, 16 - 18 December 1998*, Balkema, pp 19-25.
KNIGHT, D.W., 1999, ''Flow mechanisms and sediment transport in compound channels'', *Proc. 1st Sino-US Workshop on Sediment Transport and Disasters*, 15-17 March, Special Issue of International Journal of Sediment Research, [Eds Z. Y. Wang, T. W. Soong, & B.C. Yen], Vol. 14, No. 2, Beijing, China, pp 217-236.
KNIGHT, D.W., BROWN, F.A., VALENTINE, E.M., NALLURI, C., BATHURST, J.C., BENSON, I.A., MYERS, W.R.C., LYNESS, J.F. & CASSELLS, J., 1999, ''The response of straight mobile bed channels to inbank and overbank flows'', *Proc. Instn of Civil Engineers, Water, Maritime and Energy*, Vol. 136, Dec. pp 211-224.
MYERS, W.R.C., and BRENNAN, E.K., 1990, ''Flow resistance in compound channels'', *Journal of Hydraulic Research,* IAHR, Vol. 28, No. 2, pp 157-155.
MYERS, W.R.C., and LYNESS, J.F., 1997, ''Discharge ratios in smooth and rough compound channels'', *Journal of the Hydraulics Division*, ASCE, Vol. 123, HY3, No. 3, March, pp 182-188.
MYERS, W.R.C., KNIGHT, D.W., LYNESS, J.F., and CASSELLS, J., and BROWN, F.A.., 1999, ''Resistance coefficients for inbank and overbank flows'', *Proc. Instn of Civil Engineers, Water, Maritime and Energy*, Paper 11788, Vol. 136, June, pp 105-115.
MYERS, W.R.C., LYNESS, J.F., and CASSELLS, J., 2001, ''Influence of boundary roughness on velocity and discharge in compound river channels'', *Journal of Hydraulic Research,* IAHR, Vol. 39, No. 2, pp. 311-320.
NORDIN, C.F., 1971, ''Statistical properties of dune profiles'', USGS Professional Paper, 562-F.
SELLIN, R.H.J., 1964, '', A laboratory investigation into the interaction between the flow in the channel of a river and that over its floodplain'', *La Houille Blanche*, No. 7, pp 793-803.
SHIONO, K. and KNIGHT, D.W., 1991, ''Turbulent open channel flows with variable depth across the channel'', *Journal of Fluid Mechanics,* Vol. 222, pp 617-646 (and Vol. 231, October, p 693).
VALENTINE, E.M., BENSON, I.A., NALLURI, C. & BATHURST, J.C., 2001, ''Regime theory and stability of straight channels with bankfull and overbank flow'', *Journal of Hydraulic Research,* IAHR, Vol. 39, No. 3, pp. 259-268.
VAN RIJN, L.C., 1984, ''Sediment transport, part III : bed forms and alluvial roughness'', *Journal Hydraulic Engineering,* ASCE, Vol. 110, No. 12, December, pp 1733-1754.
WALLIS, S.G. and KNIGHT, D.W., 1984, ''Calibration studies concerning a one-dimensional numerical tidal model with particular reference to resistance coefficients'', *Estuarine, Coastal and Shelf Science*, Academic Press, London, No. 19, pp 541-562.
WHITE, W.R., PARIS, E., and BETTESS R., 1980, ''The frictional characteristics of alluvial streams : a new approach'', *Proc. Instn Civ.Engrs,* Part 2, Vol. 69, Sept., pp 737-750.
WORMLEATON, P.R., 1996, ''Floodplain secondary circulation as a mechanism for flow and shear stress redistribution in straight compound channels'', In *Coherent Flow Structures in Open Channels* [Eds Ashworth, Bennett, Best & McLelland], Chapter 28, J Wiley, pp 581-608.
YEN, B.C., 1992, ''Hydraulic resistance in open channels'' *in Channel Flow Resistance: Centennial of Manning's Formula*, [Ed. B.C. Yen], Water Resources Publications, Colorado, USA.